Jurnal Teknologi

Full Paper

SEISMIC BEHAVIOR OF MULTI-STORIED RC BUILDING WITH RE-ENTRANT CORNER

Md. Nazmul Hassan, Sharmin Reza Chowdhury*, Raisul Islam Shuvo

Department of Civil Engineering, Ahsanullah University of Science and Technology, 141 & 142, Love Road, Tejgaon Industrial Area, Dhaka, Bangladesh

Article history
Received
28 June 2023
Received in revised form
5 October 2023
Accepted
5 October 2023
Published Online
18 February 2024

*Corresponding author
chowdhury.ce@aust.edu

Graphical abstract

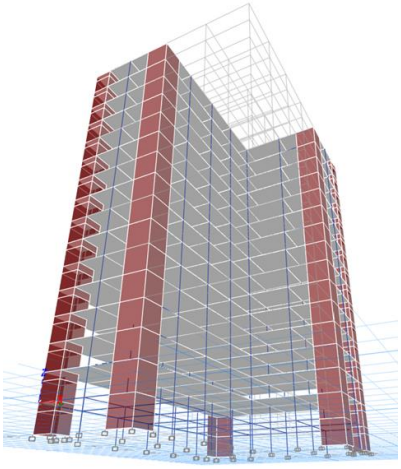

Abstract

Nowadays, buildings often feature irregular floor plans for functional, aesthetic, or economic reasons. Constructing earthquake-resistant structures in seismic areas, especially with irregular shapes like re-entrant corners, poses challenges. Such corners are common when maximizing limited space is a priority. In earthquakes, re-entrant corners in structures pose major vulnerabilities, causing stress concentration and torsion problems. The main aim of this paper is to develop finite element structural analysis models of 10, 12, and 15-storied L-shaped RC buildings with a re-entrant corner under different seismic zones using equivalent static analysis (ESA) and response spectrum analysis (RSA). This research also focuses on the overall behavior of analysis results (story drift, overturning moment, base shear, etc.) with the influence of re-entrant corner. It also investigates the performance of columns and beams near re-entrant corners as the number of stories increases in different seismic zones. For the current study, ETABS V19 is used. Models consider seismic, dead, and live loads. The Bangladesh National Building Code (BNBC) 2020 is used to examine the equivalent static analysis (ESA) and the response spectrum analysis (RSA) methods. It has been concluded from the study that re-entrant corner beams consistently exhibit the highest bending moments and torsion levels across all seismic zones. Similarly, re-entrant corner columns consistently demand the most axial force and rebar when compared to similar column types. Furthermore, the study identifies maximum stress levels in re-entrant corner slabs across all seismic zones.

Keywords: Re-entrant corner, Seismic zone, BNBC 2020 code, Equivalent static analysis (ESA), and Response spectrum analysis (RSA)

© 2024 Penerbit UTM Press. All rights reserved

1.0 INTRODUCTION

In recent times, many buildings have been designed with irregular configurations. The irregular configuration of buildings has been one of the major issues to be addressed, for those located in earthquake-prone areas [1]. Past and recent earthquake events demonstrate that buildings with irregular configurations are more vulnerable to earthquake damage [2]. An RC building that is unsymmetrical and has a lack of continuity in geometry, mass, or load-resisting elements is called an irregular building. Building irregularities come in many different forms. One of these is the re-entrant corner irregularity. Buildings with re-entrant corners are common when there is a desire to maximize the utilization of the smallest amount of space available. Furthermore, these buildings respond differently when placed in different seismic zones. The presence of re-entrant corners in buildings is one of the key weaknesses in the event of an earthquake,

causing stress concentration and torsion-related complications [3]. For this reason, it is necessary to investigate re-entrant corner building more and more.
One of the most devastating natural catastrophes is an earthquake. Bangladesh is situated in an area that is seismically active. It is situated where multiple active tectonic plates/fault boundaries cross, which has recently been the site of many earthquakes. In actuality, earthquakes of magnitudes 6.0–7.0 have struck the divisions of Dhaka, Mymensingh, Rangpur, Chattogram, and Sylhet, while earthquakes of magnitudes 5.0–6.0 have struck the divisions of Khulna and Rajshahi [4]. The country's upper center and northwest areas, from Sylhet to Chattogram, are in a high seismic zone, but Dhaka is located in a moderate zone. Bangladesh is in a moderate to a high seismic danger zone, according to worldwide seismic hazard maps, with a maximum peak ground acceleration of 0.25g and a 10% chance of exceeding it in the next 50 years [5].

Until 1993, Bangladesh had no specific building code for seismic analysis, design, or details. The Housing and Building Research Institute (HBRI), commonly known as BNBC, released the Bangladesh National Building Code (BNBC) in 1993 [6]. The BNBC's seismic design guidelines were based on the Uniform Building Code (UBC). After that, structural engineers started using BNBC on a large scale. The Bangladesh National Building Code (BNBC) 2020 was gazetted by the government of the People's Republic of Bangladesh in February 2021 as a necessary norm for building design and construction.

In recent years, the growth of RC irregular structures has accelerated, particularly in Dhaka. During an earthquake, the most common source of damage to reinforced concrete (RC) frame buildings is uneven building arrangements [7]. An irregular building is a reinforced concrete structure that is asymmetrical and lacks continuity in mass, geometry, or load-bearing elements.

The existence of re-entrant corners is one of the key problems in buildings in the event of an earthquake. Re-entrant corner structures are typically built when there is an opportunity to make the most of the available space. A re-entrant corner is known as a "plan Irregular Structure". Due to its useful and visually beautiful design, this type of construction is increasingly gaining popularity. It also provides sufficient sunlight and ventilation, which are very essential in urban life [8].

A lot of research and inquiry has been done in order to better understand the behavior of re-entrant corner irregular structures and improve their performance. Re-entrant corner irregular buildings must also be carefully constructed according to new seismic requirements. The goal of this research is to evaluate the seismic performance of re-entrant corner RC moment-resisting frame buildings with 10, 12, and 15- stories in compliance with BNBC 2020.

The study's goal is to evaluate the seismic behavior of re-entrant corner irregular RC moment-resistant frame structures using a range of static and response spectrum analysis methodologies. For this purpose, the following objectives are set for this study:

- To create finite element structural analysis models for L-shaped RC buildings (10-, 12-, and 15-stories) featuring a re-entrant corner in various seismic zones using equivalent static analysis (ESA) and response spectrum analysis (RSA).
- To assess the impact of the re-entrant corner on analysis results (such as story drift and base shear etc.) and understand the overall behavior.
- To compare the behavior of the columns and beams near the re-entrant corner with an increasing number of stories in different seismic zones.

The entire process is executed in accordance with the methodology outlined in the flowchart.

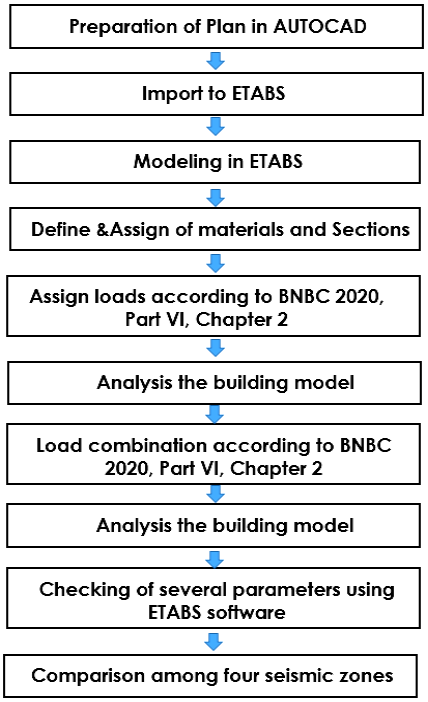

Figure 1 Flowchart of the research methodology

2.0 HISTOLOGICAL ANALYSIS ON RE-ENTRANT CORNER AND EARTHQUAKE

Damage to re-entrant corners of structures is generally acknowledged following the earthquakes that occurred in Mexico City in 1985, the Alaska earthquake in North America in 1964, the Santa Barbara earthquake in California in 1925, and the Kanto earthquake in Japan in 1923 [9].

Damage to the structure happened first in the re-entrant corner in some of these key incidents, and subsequently spread to other portions of the building [10]. The West Anchorage High School in Alaska was extensively damaged in the 1964 earthquake, highlighting the risks of construction with re-entrant corners (Figure 1). In this image, the notch of this

spread L-shape structure has been damaged. After the 1985 earthquake in Mexico City, damage to the roof diaphragm and upper floors radiating out from the re-entrant corner of the Ministry of Telecommunication building was visible (Figure 2).

Figure 1 West Anchorage High School in Alaska sustained damage to its roof diaphragm at the re-entrant corner during the 1964 earthquake [11]

Figure 2 The upper floors and re-entrant corner of Mexico City's Ministry of Telecommunications Building were damaged during the 1985 earthquake [12]

Many researchers carried out different analysis on Re-entrant corner. Shreyasvi and Shivakumaraswamy (2015) [11] carried out that the columns at the re-entrant corners are subjected to greater earthquake stresses than other interior columns. The columns need more ductile detailing as compared to ordinary columns. Furthermore, the greater the force experienced by the column at the re-entrant corner, the longer the structure's cantilever projection from the re-entrant corner.

Kumar *et al*. (2017) [13] performed an analysis by FEM software ETABS of an L-shaped building structure with a re-entrant corner, and it was discovered that the influence of variation in base shear was greater in a 15-storied building than in a 10-or 20-storied building in the same soil type (soil type 2) in all IS code zones.

Ankon (2020) [14] studied the L-shaped building and was determined to be the most susceptible in both directions when compared to other building forms. The response spectrum with the greatest displacement among all loads is found. In addition, irregular structures were shown to be more vulnerable to wind loads than regular buildings in the investigation.

3.0 STRUCTURAL MODELING & ANALYSIS

Finite element modeling of structural systems is essential for the design of structures and the evaluation of their performance. ETABS, a structural analysis and design integrated tool, is utilized in this work. The analytical methodologies and key factors used in equivalent static (ESA) and response spectrum (RSA) analysis are shown in this portion.

3.1 Consideration of Building Structures for the Study

3.1.1 Building Models' Structural Geometry

The effects of seismic behavior for 10, 12, and 15-storied hypothetical buildings with re-entrant corners are investigated in this study. As shown in Figure 3, all of the structures have the same symmetrical plan configuration with four bays in the X direction and six bays in the Y direction. The "bay width" has been determined to be 20 feet. Re-Entrant Corner Check:

Ax/Lx= (40/80) =0.50>0.15, Ay/Ly= (40/120)=0.33>0.15 [11]

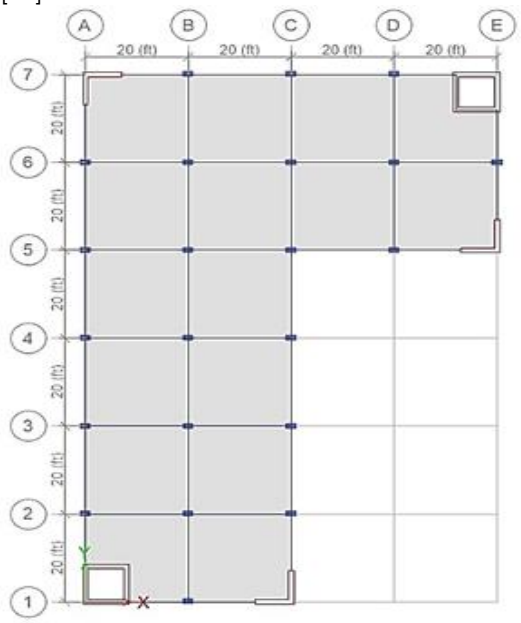

Figure 3 Plan view of the study building

3.1.2 Building Analysis Parameters

An RC building is designed where 10, 12 and 15 number of stories are considered. The remaining typical and bottom story height is 10 feet. Column size for 10, and 12 storey is considered 15"x25" and for 15 storey is considered 15"x30" (Outside) & 15"x40" (Inside). The shear wall and slab thickness are considered 12" and 6". According to BNBC 2020, all the analyses are done at seismic zone I, II, III, and IV.

For these 4 zones, the zone coefficient are 0.12, 0.20, 0.28, and 0.36. For this analysis, the Compressive strength of concrete and the yield strength of steel are considered as 4000 psi and 60,000 psi respectively. Figure 4 illustrates some key parameters in building.

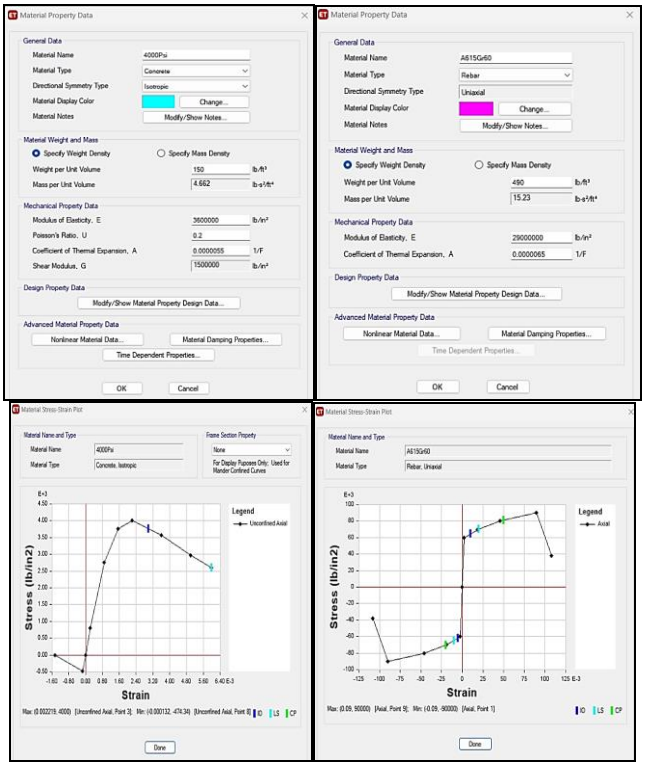

Figure 4 Some Building analysis parameters

The ultimate strength design (USD) approach is used to develop the structural member. In this analysis, the structure's dead load scenario is limited to the self-weight of beams, columns, slabs, floor finish, and masonry infill walls. The partition wall load is 25 psf, while the total vertical load for the structure's floor finish is 20 psf. In this study, the live load (LL) that has been applied to the floor levels is 42 psf, and the roof live load (Lr) is 100 psf. When calculating seismic weight, a 25% live load is taken into account. Additional criteria are used in the seismic load calculation according to BNBC 2020 (sec. 2.5.7.3). Table 1 shows the summary of building analysis parameters.

Table 1 Building analysis parameters

Type of occupancy	RC Building
Geometric parameters:	
Foundation level to ground level	10 Feet
Number of bays-X direction	4 Nos
Number of bays-Y direction	6 Nos
Spacing of bays-X direction	20 Feet
Spacing of bays-Y direction	20 Feet
Height of each storey	10 Feet
Number of storey	10, 12, and 15
Dimensions of structural members:	
Floor Beam cross-section	12"x24"
Grade Beam cross-section	12"x18"
Column cross-section	10 Storey Building:15"x25" 12 Storey Building:15"x25" 15 Storey Building:15"x30" (Outside) and 15"x40" (Inside)
Slab Thickness	6"
RCC Wall	12"
Material:	
Compressive strength of concrete, f'_c	4,000 Psi
Modulus of elasticity of concrete, E_c	3,600 Psi
Poisson's ratio	0.20
Yield stress of steel, f_y	60,000 Psi
Seismic Parameters:	
Seismic zone	I, II, III, and IV
Seismic Zone coefficient, Z	0.12, 0.20, 0.28, 0.36
Importance Factor, I	1.00
Response reduction factor, R	7
System over strength factor, Ω	2.5
Deflection amplification factor, C_d	5.5
Type of soil	C Type
Ct (Concrete moment-resisting frames)	0.016 (FPS Unit)
T (Time Period)	1.10 sec, 1.27 sec, and 1.54 sec

3.2 Earthquake Load Analysis

A number of seismic analysis methodologies are presented in BNBC-2020. The appropriate static analysis and response spectrum analysis are done in this investigation.

3.2.1 *Equivalent Static Analysis (ESA)*

It assumes that the building responds in its fundamental mode. The distributed forces are then used to determine the story displacements and internal forces, such as, bending moment, shear, torsion, etc. at various structural components [15]. Figure 5 illustrated the Fundamental concepts of Equivalent static analysis (ESA).

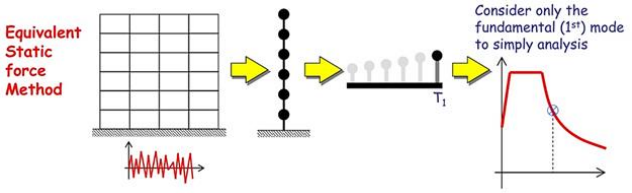

Figure 5 Fundamental concepts of Equivalent static analysis (ESA)

3.2.2 *Response Spectrum Analysis (RSA)*

Response-spectrum analysis (RSA) is a linear-dynamic analysis method. Different modes represent the

maximum response of the displacement pattern [16]. Figure 6 illustrated the Fundamental concepts of Response spectrum analysis (RSA).

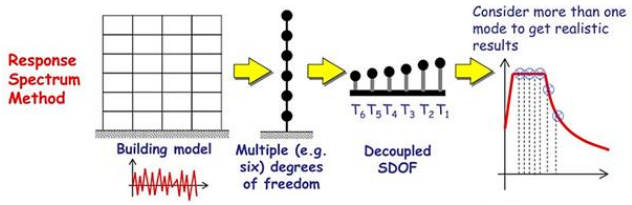

Figure 6 Fundamental concepts of Response spectrum analysis (RSA)

4.0 RESULTS & DISCUSSIONS

This section includes discussions of storey drift, storey shear, overturning moment, storey displacement, column service and axial force, column and beam moments, column rebar percentage, and torsion. Different parametric studies will be carried out to see the effect of re-entrant corners on the behavior of buildings.

4.1 Storey Drift

The level x inelastic deflections in this section are calculated using the following recommended equation by BNBC 2020:

$$\delta_X = \frac{C_d \delta_{xe}}{I}$$

Where C_d is the deflection amplification factor and δ_{xe} is the deflection determined from elastic analysis [17]. The letters I stand for Importance Factor. According to BNBC 2020, C_d and I are calculated in this investigation as 5.5 and 1.0, respectively.

The difference between the deflections at the top and bottom of the storey under consideration was used to calculate the design storey drift at storey x as follows: $\Delta_x=\delta_x-\delta_{(x-1)}$

Table 2 shows the Maximum storey drift in various seismic zones. For the 10, 12, and 15-storied buildings in Figure 7, the static analysis (ESA) storey drifts along the X-direction are shown, whereas the response spectrum analysis (RSA), is shown in Figure 8.

Table 2 Maximum storey drift in various seismic zones

Storey	Zone	X-Direction			Y-Direction		
		ESA	RSA	Difference in storey Drifts (%)	ESA	RSA	Difference in storey Drifts (%)
10	1	0.444	0.392	11.65%	0.457	0.430	5.84%
	2	0.741	0.654	11.65%	0.761	0.717	5.84%
	3	1.037	0.916	11.64%	1.066	1.004	5.85%
	4	1.333	1.178	11.65%	1.371	1.291	5.84%
12	1	0.484	0.404	16.50%	0.493	0.440	10.82%
	2	0.808	0.680	15.77%	0.822	0.733	10.81%
	3	1.131	0.952	15.77%	1.151	1.027	10.81%
	4	1.454	1.225	15.77%	1.480	1.320	10.81%
15	1	0.484	0.375	22.39%	0.491	0.394	19.74%
	2	0.806	0.626	22.38%	0.819	0.657	19.73%
	3	1.129	0.876	22.38%	1.146	0.920	19.72%
	4	1.452	1.127	22.39%	1.474	1.183	19.74%

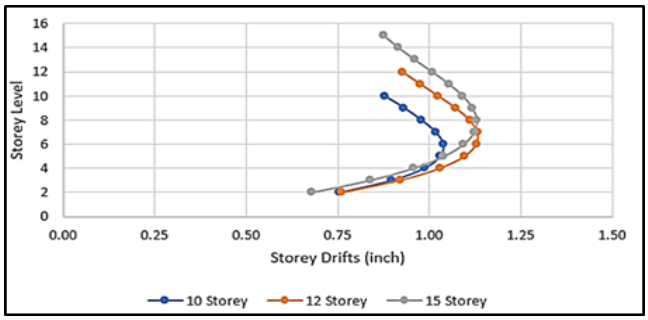

Seismic Zone 3

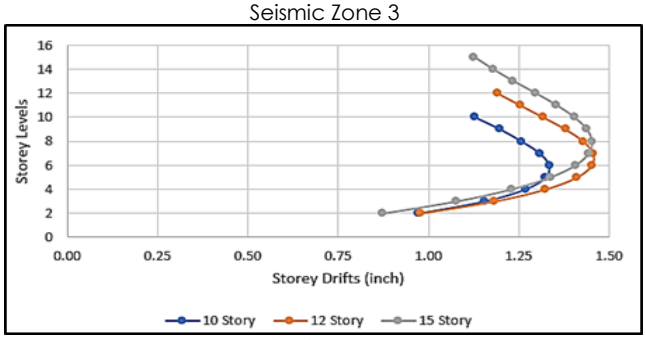

Seismic Zone 4

Figure 7 Storey drifts for different storey in ESA (X-direction)

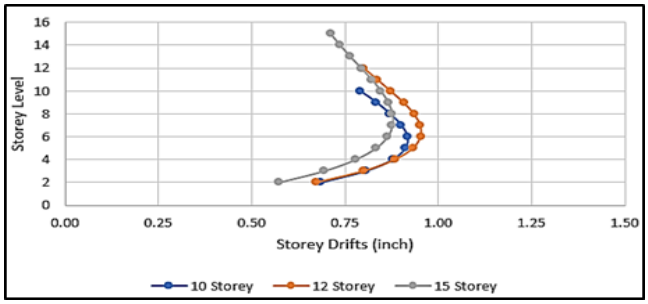

Seismic Zone 3

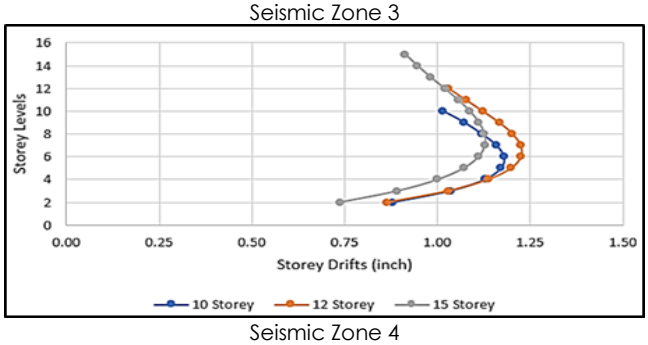

Seismic Zone 4

Figure 8 Storey drifts for different storey in RSA (X-direction)

Storey drift is displayed higher for ESA rather than RSA for all seismic zones which are found from Figures 7 to 8. The rate of increasing storey drift is observed when increasing with building height in both X & Y-direction. Once more, as the seismic zone is increased, higher story drifts for buildings of the same height are found. All of the buildings' design drifts are found to be within the BNBC 2020 code's permitted drift limit.

4.2 Storey Shears

Storey shears from equivalent static analysis (ESA) and response spectrum analysis (RSA) are estimated for 10, 12, and 15-storied RC frame buildings. The comparison of storey shears using ESA and RSA techniques is shown in Figures 9 and 10.

It is seen from figures that total base shear increases with buildings having higher heights. It has been noted that the base shear of the structure is influenced by the zoning coefficient value. Also, RSA base shear values are obtained above 85% of the ESA base shear (same in this study). The outcomes are thus satisfactory, as mentioned in BNBC 2020 (sec. 2.5.9.4).

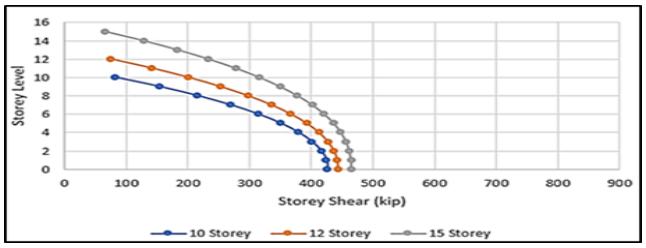

Seismic Zone 2

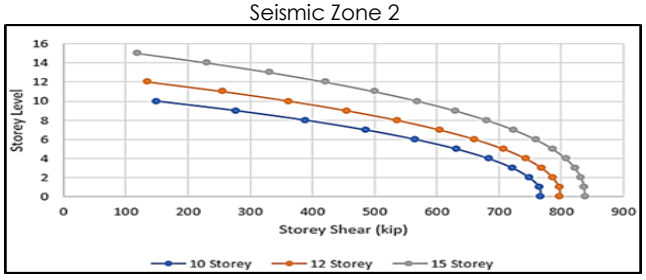

Seismic Zone 4

Figure 9 Storey shear for different storey in ESA

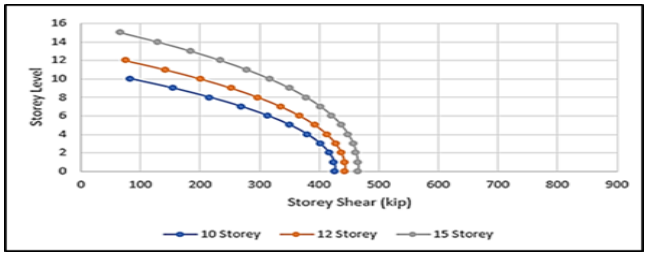

Seismic Zone 2

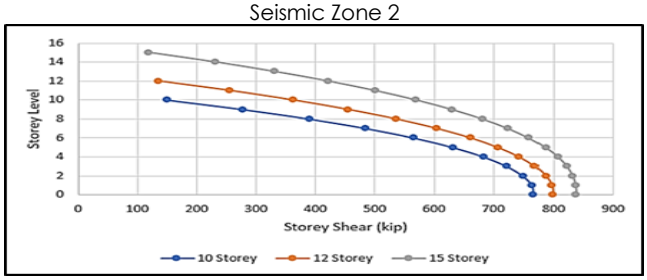

Seismic Zone 4

Figure 10 Storey shear for different storey in RSA

4.3 Overturning Moment

The overturning moments (BNBC 2020, sec. 2.5.7.8) at level x, Mx, shall be determined as follows:

$$M_x = \sum_{i=0}^{n} F_i\,(h_i - h_x)$$

Where, Fi=Portion of the seismic base shear, V induced at level I. hi, hx=Height from the base to level i or x [18]. The results of the overturning moment's calculation using the BNBC 2020 code are listed in Table 3. Also, Figures 11 and 12 compare the overturning moment as determined by ESA and RSA.

Table 3 Overturning moments (OM) in various seismic zones

Zone	10 Storey		Difference in OM (%)	12 Storey		Difference in OM (%)	15 Storey		Difference in OM (%)
	ESA	RSA		ESA	RSA		ESA	RSA	
	kip-ft	kip-ft		kip-ft	kip-ft		kip-ft	kip-ft	
1	20473	20280	0.94%	25295	24672	2.46%	32969	31078	5.74%
2	34122	33800	0.94%	42159	41120	2.46%	54948	51796	5.74%
3	47771	47320	0.94%	59023	57568	2.46%	76927	72515	5.74%
4	61420	60841	0.94%	75887	74016	2.46%	98906	93233	5.74%

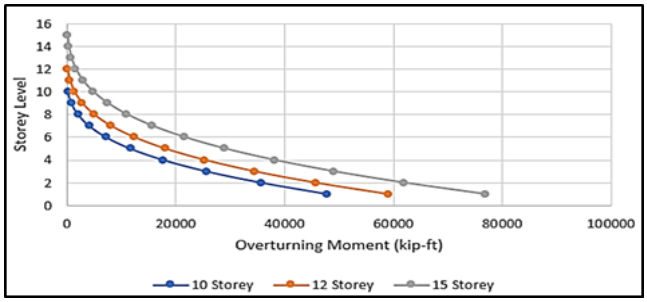

Seismic Zone 3

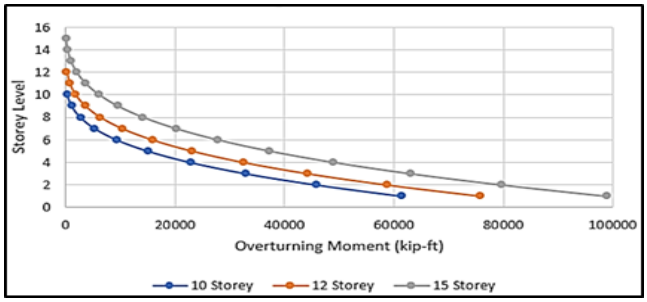

Seismic Zone 4

Figure 11 Overturning moments for different storey in ESA

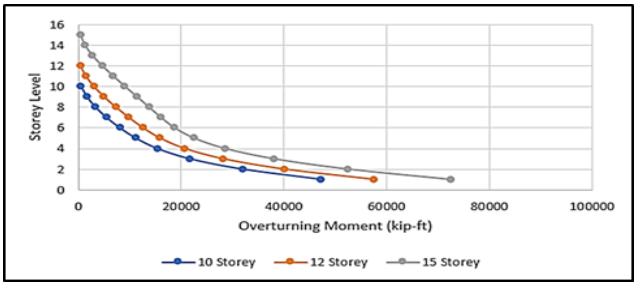

Seismic Zone 3

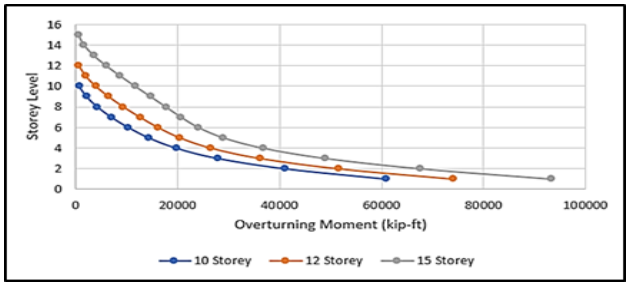

Seismic Zone 4

Figure 12 Overturning moments for different storey in RSA

For buildings with rising heights, the ESA is shown to have more overturning moments than the RSA in various seismic zones. The total overturning moment varies across all zones for all buildings. The overturning moment of this structure is observed to be influenced by the seismic zone coefficients as well as building height. At 10, 12, and 15-storied buildings, the RSA overturning moments are all shown to be less than the ESA, by 0.94%, 2.46%, and 5.74%, respectively.

4.4 Storey Displacement

The storey displacement values for ESA and RSA are displayed in Tables 4. The maximum storey displacement is found in the roof for all seismic zones in buildings, both in the X and Y directions.

The storey displacement discovered in both directions for the 10, 12 and 15-story buildings for ESA and RSA at zone 4 is presented in Figures 13 and 14.

Table 4 Storey displacement in various seismic zones (X and Y direction)

Direction	Zone	10 Storey		Difference in Storey Displacement	12 Storey		Difference in Storey Displacement	15 Storey		Difference in Storey Displacement
		ESA inch	RSA inch		ESA inch	RSA inch		ESA inch	RSA inch	
X	1	0.73	0.65	10.96%	0.93	0.80	13.98%	1.13	0.90	20.35%
	2	1.21	1.08	10.74%	1.55	1.33	14.19%	1.89	1.51	20.11%
	3	1.69	1.51	10.65%	2.17	1.86	14.29%	2.65	2.11	20.38%
	4	2.18	1.95	10.55%	2.79	2.40	13.98%	3.4	2.71	20.29%
Y	1	0.74	0.71	4.05%	0.95	0.86	9.47%	1.15	0.95	17.39%
	2	1.24	1.18	4.84%	1.58	1.43	9.49%	1.92	1.59	17.19%
	3	1.73	1.65	4.62%	2.21	2.01	9.05%	2.69	2.22	17.47%
	4	2.23	2.12	4.93%	2.84	2.58	9.15%	2.85	2.85	17.39%

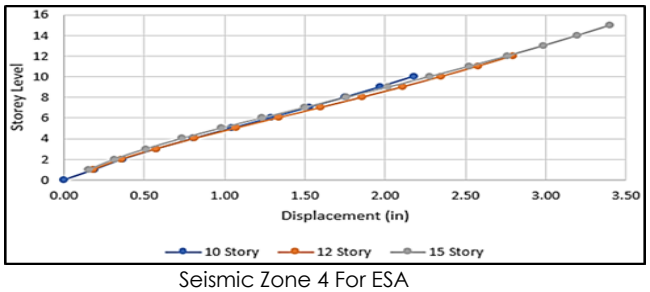

Seismic Zone 4 For ESA

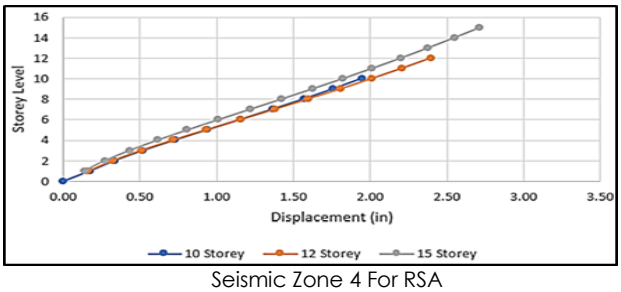

Seismic Zone 4 For RSA

Figure 13 Storey displacement for different storey in ESA and RSA for zone 4 (X-direction)

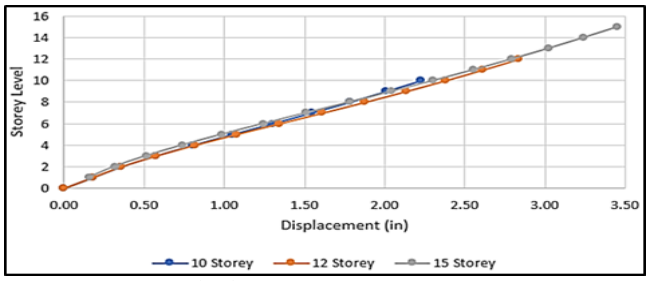

Seismic Zone 4 For ESA

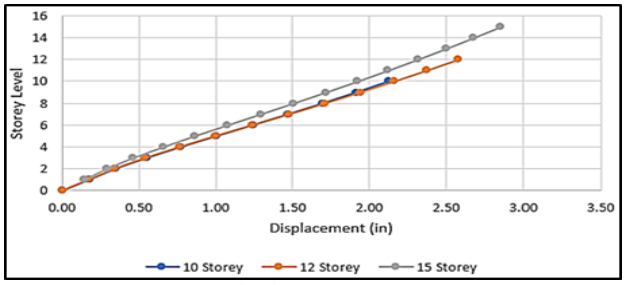

Seismic Zone 4 For RSA

Figure 14 Storey displacement for different storey in ESA and RSA for zone 4 (Y-direction)

For buildings with rising heights, the ESA is shown to have more storey displacement than the RSA in various seismic zones. The rate of increasing storey displacement is observed when increasing with building height in both X and Y-directions. Also, the increasing rate is observed for the same building when changing the seismic zone coefficient. All of the structures' displacements are found to be within the BNBC 2020 code's permitted drift limit.

4.5 Examine the Selected Columns

4.5.1 Comparison of Column Service Load and Axial Force

Service load (D+L) is normally counted by both dead load and live load. The axial force (D+L+EQ) is considered by the dead load, live load, and seismic load [19]. In this study, Table 5 shows the axial force of ESA and RSA for the 3C, 5C (re-entrant corner column), and 7C columns. The selection of columns is marked in Figure 15 for observation.

The re-entrant corner column (5C) has been observed to have the highest service and axial force in both the ESA and RSA for all seismic zones. From the above study, the re-entrant corner column (5C) is found to be more critical than other columns.

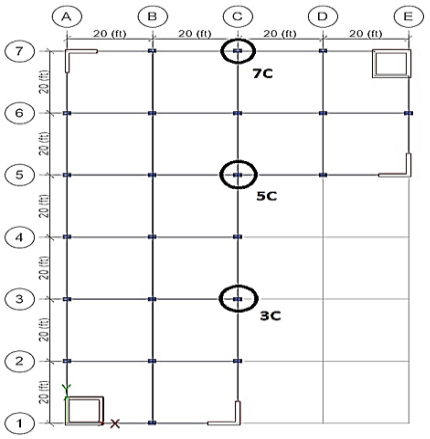

Figure 15 3C, 5C, and 7C selected columns' locations

Table 5 Axial Force by ESA and RSA

Zone	Storey	Axial Force, Col: 7C (kip)			Axial Force, Col: 5C (kip)			Axial Force, Col: 3C (kip)		
		Service Load	Combination Load		Service Load	Combination Load		Service Load	Combination Load	
			ESA	RSA		ESA	RSA		ESA	RSA
1	10	528	674	674	718	920	920	542	692	692
	12	630	808	804	851	1090	1090	650	829	819
	15	764	974	972	1000	1280	1280	796	1044	1012
2	10	528	683	684	718	920	920	542	699	700
	12	630	816	815	851	1090	1090	650	839	840
	15	764	993	989	1000	1280	1280	796	1030	1028
3	10	528	695	694	718	920	920	542	711	713
	12	630	831	829	851	1090	1090	650	854	854
	15	764	1013	1007	1000	1280	1280	796	1049	1046
4	10	528	707	706	718	930	920	542	723	724
	12	630	846	843	851	1090	1090	650	869	869
	15	764	1032	1025	1000	1280	1280	796	1068	1064

4.5.2 Comparison of Selected Column Bending Moments

The individual columns 3C, 5C, and 7C are shown in Figure 15. The static bending moments are shown in Figures 16, 17, and 18.

The 3C column has been shown to have the highest bending moment of the other columns for all seismic zones. It is observed that the selected column moments have been displayed quite close to one another in the same seismic zone when comparing ESA and RSA. Bending moments are observed more when changing the height and increasing the seismic zone.

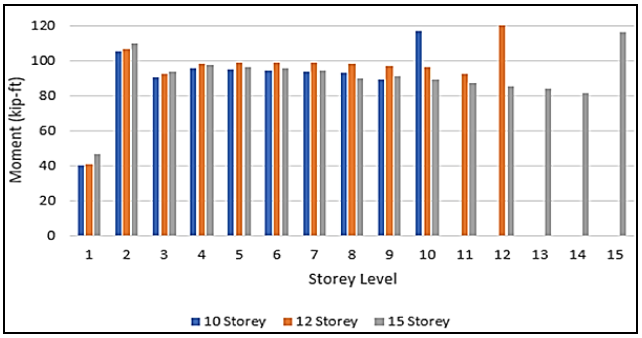

Seismic Zone 3

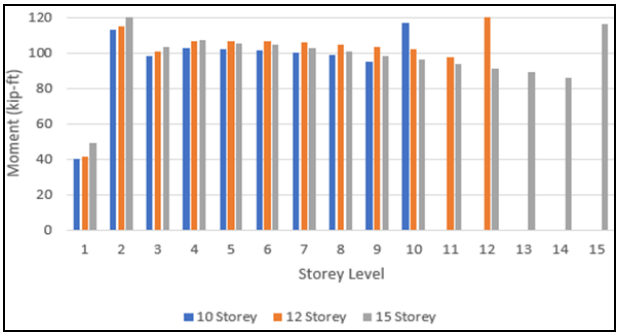

Seismic Zone 4

Figure 16 Bending moment found in ESA for 3C column

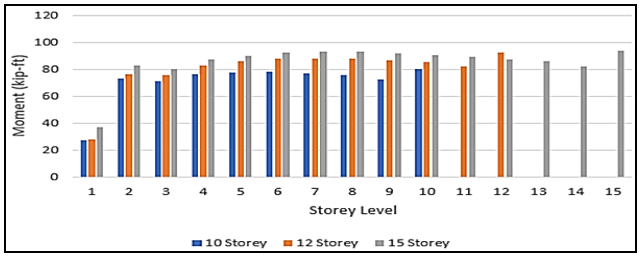

Seismic Zone 3

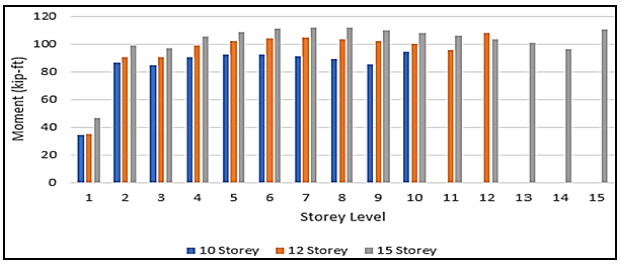

Seismic Zone 4

Figure 17 Bending moment found in ESA for 5C column

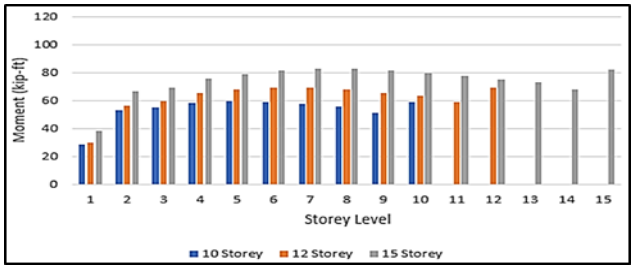

Seismic Zone 3

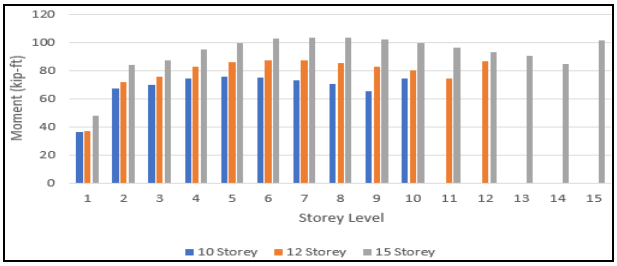

Seismic Zone 4

Figure 18 Bending moment found in ESA for 7C column

4.5.3 PMM

The PMM ratio, which represents the demand compared to capacity, encompasses both the axial force demand/capacity ratio and the bending moment demand/capacity ratio. In this context, a PMM value exceeding one will signify members that are under overstressed. The value of PMM ratio should be ≤ 1.

Figure 19 shows the demand capacity ratio of columns based on PMM for different level of re-entrant irregularity. From Figure 19 shows that the the demand capacity ratio of columns based on PMM is less than 1. So, the member is not overstressed.

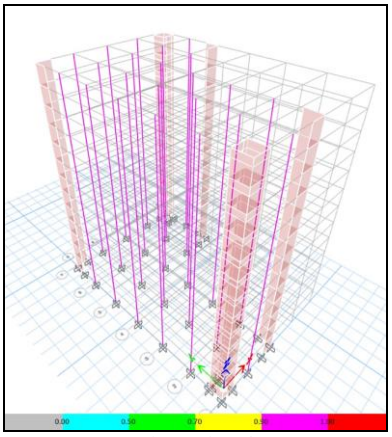

Figure 19 Demand capacity ratio of columns based on PMM

4.5.4 Requirements for Column Rebar (%)

The individual columns 3C, 5C (re-entrant corner column), and 7C are shown in Figure 15. The static analysis of the column rebar is shown in Figures 20, 21 and 22.

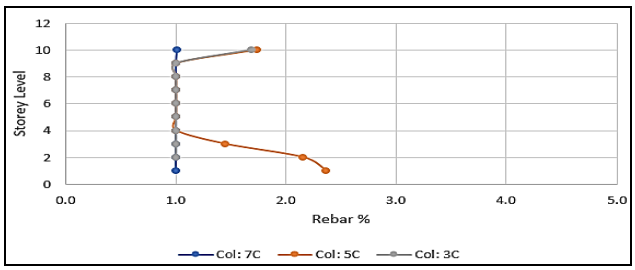

Seismic Zone 3

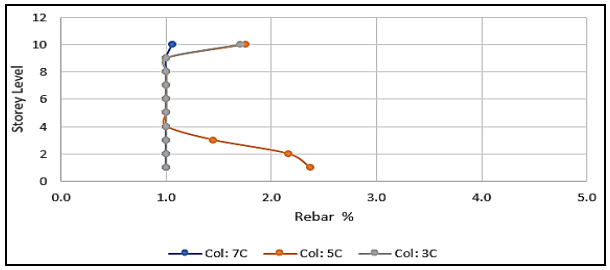

Seismic Zone 4

Figure 20 Requirements for column rebar (%) found in a 10- storied building by ESA

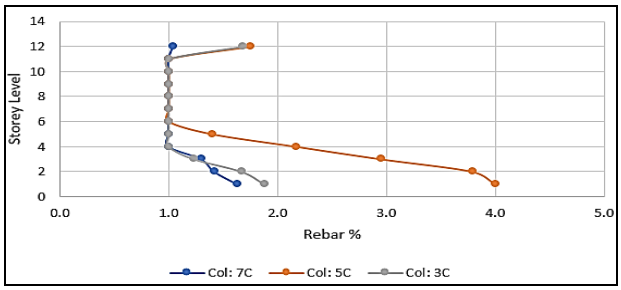

Seismic Zone 3

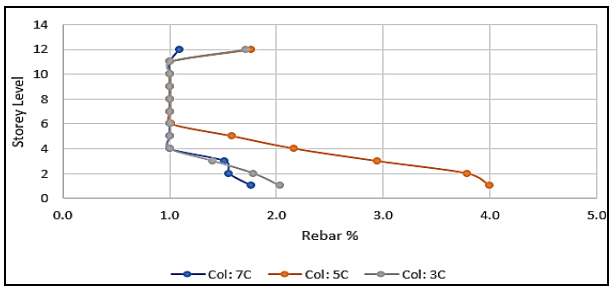

Seismic Zone 4

Figure 21 Requirements for column rebar (%) found in a 12- storied building by ESA

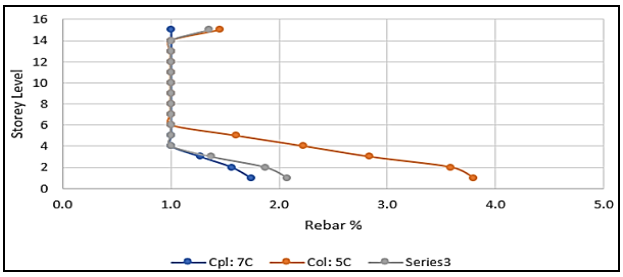

Seismic Zone 3

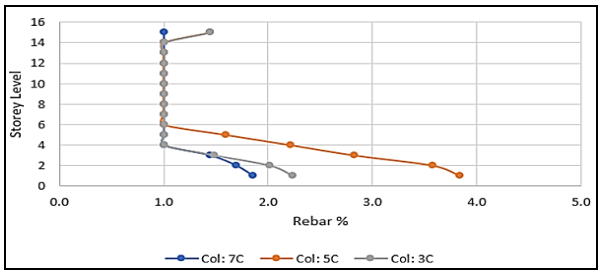

Seismic Zone 4

Figure 22 Requirements for column rebar (%) found in a 15- storied building by ESA

Due to high axial force and service load, the re-entrant corner column (5C) has a higher rebar requirement than the 3C and 7C columns. The column rebar percentage is once again readily apparent at the top level as a result of an unbalanced moment. For 10 and 12-storied buildings in the same configuration and 15-story buildings, the columns are used in a higher configuration.

4.5.5 Requirements for re-entrant corner column rebar (%)

The individual re-entrant corner column 5C is shown in Figure 15. Figure 23 has shown the re-entrant corner column rebar percentage requirements found in ESA, while Figure 24 has shown the RSA of the re-entrant corner column rebar percentage requirements found in RSA.

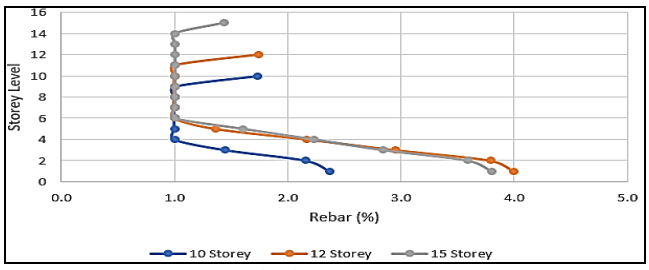

Seismic Zone 2

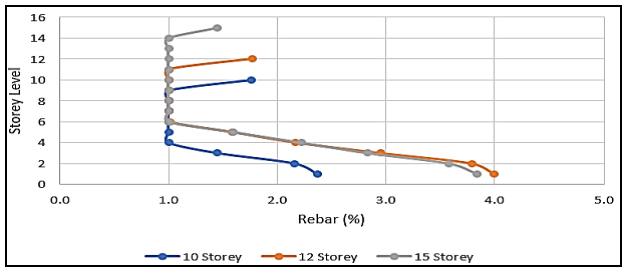

Seismic Zone 4

Figure 23 Requirements for re-entrant corner column rebar (%) by ESA

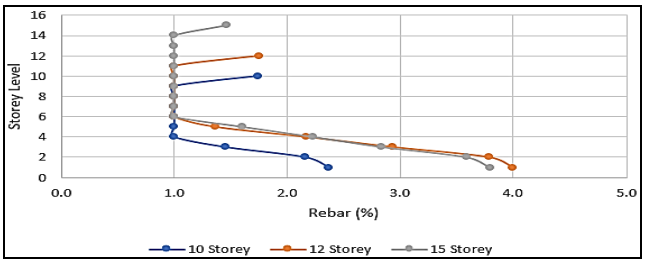

Seismic Zone 2

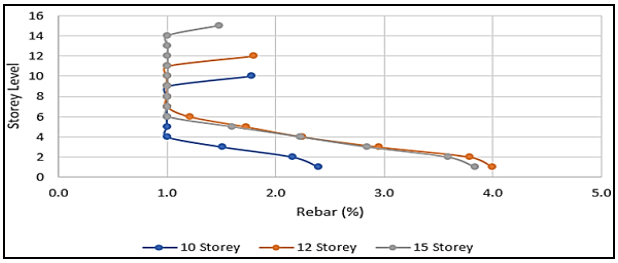

Seismic Zone 4

Figure 24 Requirements for re-entrant corner column rebar (%) by RSA

Due to the high axial and service load at the bottom, the rebar percentage of re-entrant corner columns (5C) is the highest at the bottom for all zones. However, when height increases, it is slowly decreasing [20]. Due to an unbalanced moment at the top, the column rebar percentage is higher at the top level. The 12-story building has the highest rebar percentage because the 10 and 12 storied buildings are considered to have the same column configuration, whereas the 15-storied building has larger column configurations.

4.6 Examine the Selected Beams

4.6.1 Comparison of Selected Beam Bending Moment

In Figure 25 is shown the individual beams 5 (CD), 7 (CD), C (45), and A (45). Figures 26 to 27 have been provided with the static bending moments for the 9th floor of the study buildings. Beams 5 (CD) and C (45) serve as a representation of the re-entrant corner beams.

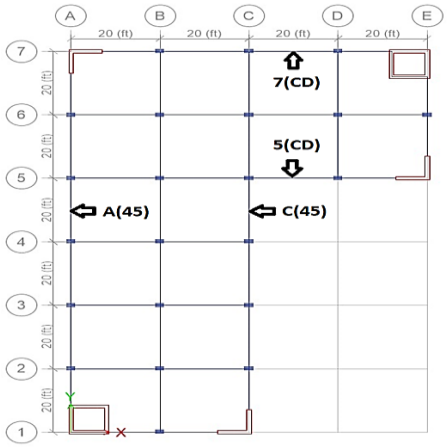

Figure 25 The beam layout for investigation

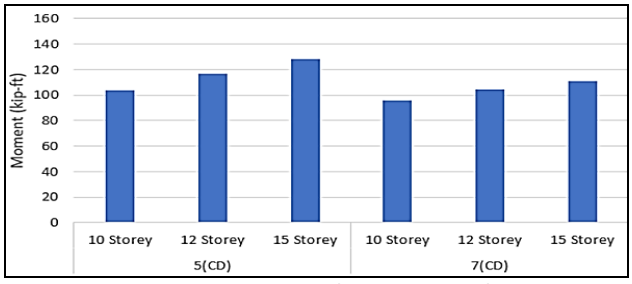

Beam 5CD & 7CD (Neg. moment)

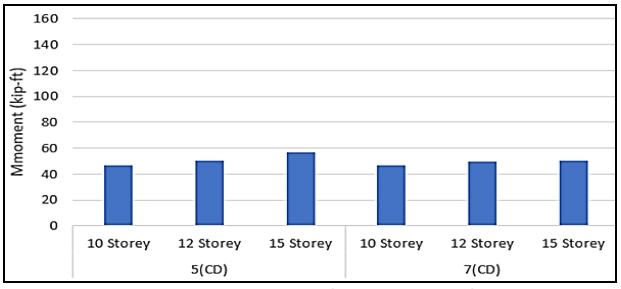

Beam 5CD & 7CD (Pos. moment)

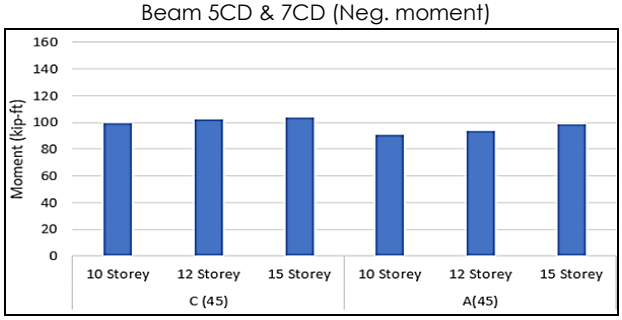

Beam C (45) & A (45) (Neg. moment)

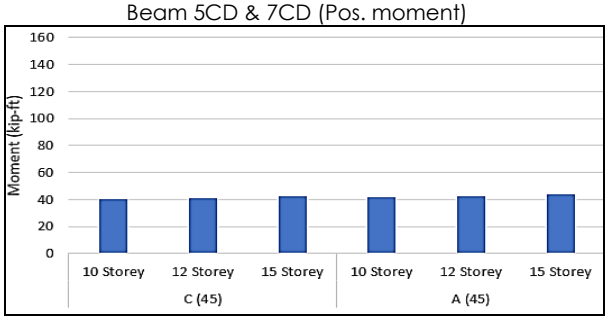

Beam C (45) & A (45) (Pos. moment)

Figure 26 5CD, 7CD, C (45), and A (45) beam bending moments found in ESA (Zone 03, 9F)

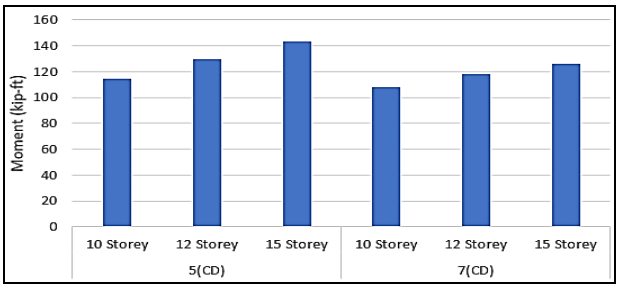

Beam 5CD & 7CD (Neg. moment)

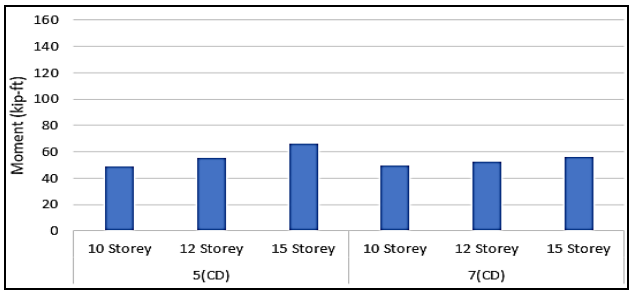

Beam 5CD & 7CD (Pos. moment)

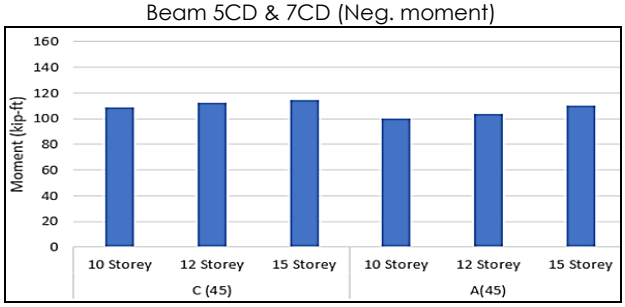

Beam C (45) & A (45) (Neg. moment)

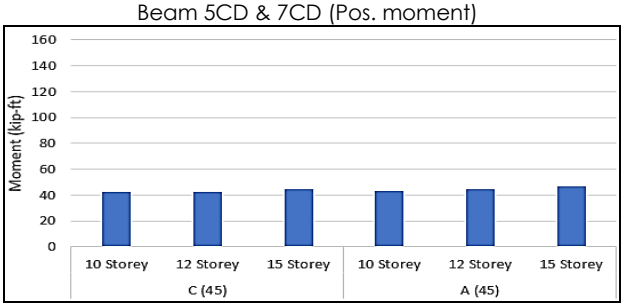

Beam C (45) & A (45) (Pos. moment)

Figure 27 5CD, 7CD, C (45), and A (45) beam bending moments found in ESA (Zone 04, 9F)

Both ESA and RSA beam moments are observed very close to each other. The maximum bending moment has been displayed for the re-entrant corner beams 5(CD) and C (45). Among these, it has been noted that beam 5(CD) has a greater bending moment.

4.6.2 Torsion of the Selected Beam

Torsion is defined as the twisting of a beam caused by a torque (twisting moment). The individual beams 5 (CD), 7(CD), C (45) and A (45) are shown in Figure 25. The static analysis and response spectrum analysis torsional moments are presented in Figures 28 to 31 for 9th floor of 10, 12, and 15 storied building.

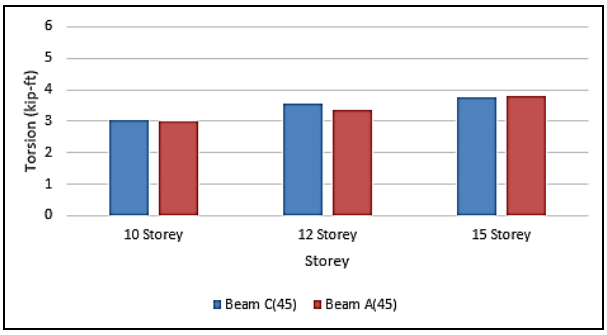

Seismic Zone 3

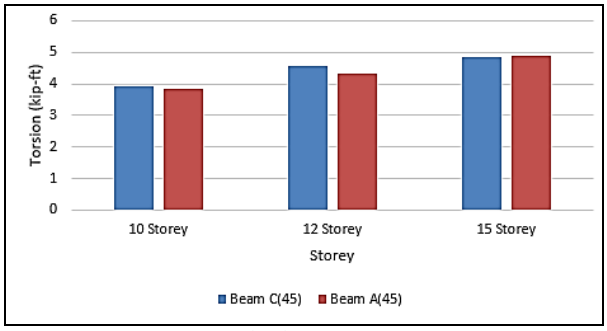

Seismic Zone 4

Figure 28 Torsion found in ESA (EQ-X, 9F)

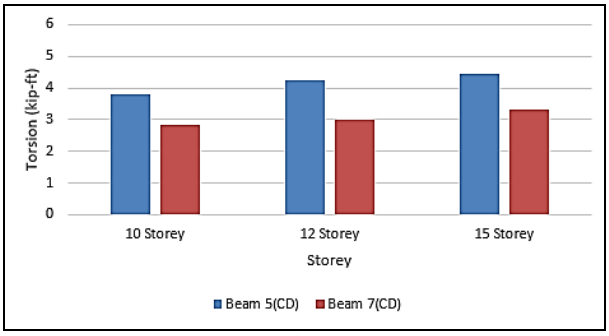

Seismic Zone 3

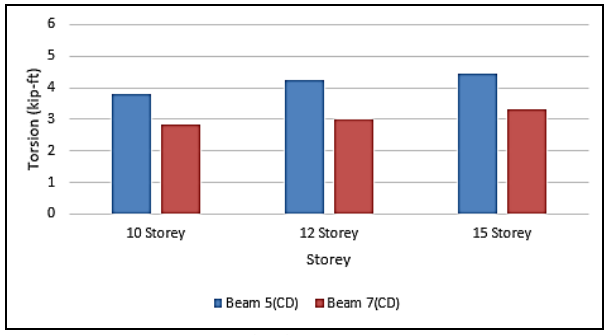

Seismic Zone 4

Figure 29 Torsion found in ESA (EQ-Y, 9F)

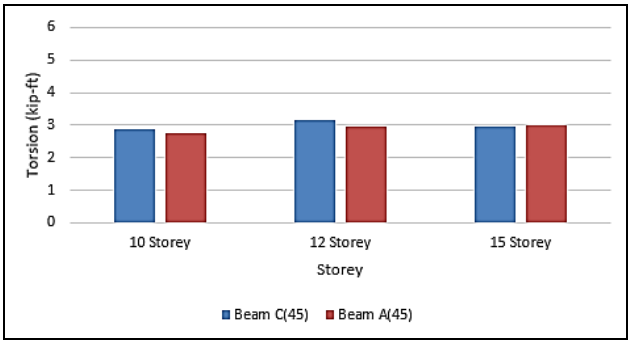

Seismic Zone 3

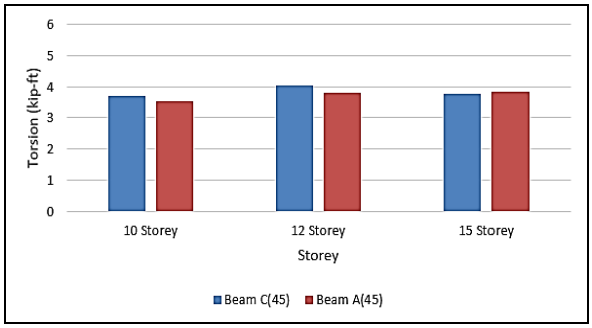

Seismic Zone 4

Figure 30 Torsion found in RSA (RS-X, 9F)

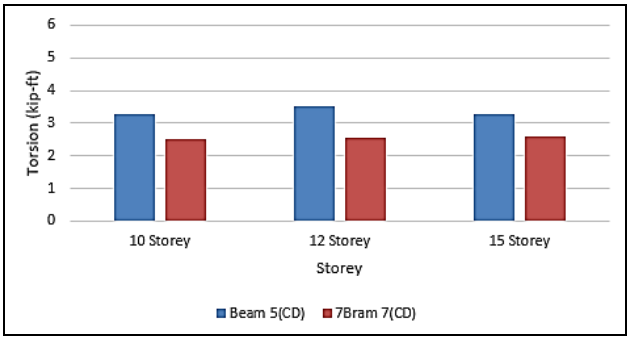

Seismic Zone 3

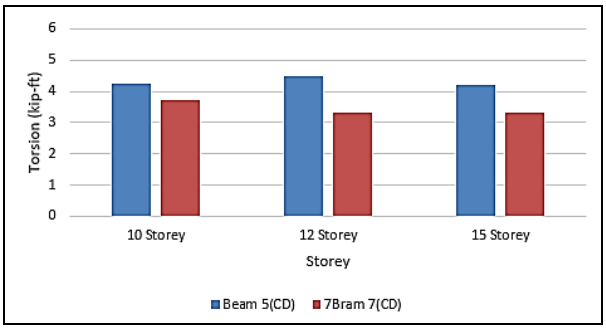

Seismic Zone 4

Figure 31 Torsion found in RSA (RS-Y, 9F)

The values of Torsion for ESA and RSA are found close to each other. A higher torsion is seen for increasing seismic zone. Zone 01 has the least torsion effect, whereas zone 04 has the most torsion in both ESA and RSA. The highest torsion effect is observed in the re-entrant corner beam 5(CD).

4.7 Modal Time Period

According to investigations into time periods, a longer modal time period is needed as a building's height rises [21]. A 15-storied building has been taken a longer time period to seismically analyze than a 10 or 12-storied building. So, 15-storied is seen as more variable when compared with 10 or 12 storied, considering a seismic time period study. The difference between the ESA and RSA modal time periods for buildings with 10, 12, and 15 storied is shown in Table 6.

Table 6 Comparision of the modal time period

Storey	Mode	T(sec),RSA	T(sec),ESA	Difference in Modal Time Period (%)
10	1	1.5	1.48	1.33
	2	1.38	1.37	0.72
	3	0.94	0.94	0.00
12	1	1.82	1.8	1.10
	2	1.67	1.65	1.20
	3	1.15	1.14	0.87
15	1	2.23	2.19	1.79
	2	1.97	1.95	1.02
	3	1.38	1.37	0.72

It has been observed that the first mode is the most vulnerable position for all buildings when compared to the second and third modes. In comparison to ESA, RSA is seen for a longer period of time when building height is taken into account. According to a dynamic study, buildings are therefore more susceptible to earthquake activity in all seismic zones as they rise in height. It is clear that dynamic analysis is necessary for successful outcomes.

4.8 Slab Stress Observation

Due to the movement of the arms, buildings with re-entrant corners are particularly vulnerable to earthquake damage [22]. This causes increased torsional forces and stress concentrations at this point as a result (Figure 32). The highest slab normal stress for the current investigation under the envelop load condition is shown in Table 7 at the re-entrant corner [23].

In all seismic zones, it has been found that the re-entrant corner slab experiences the greatest concentration of stress. Therefore, additional measures are required to prevent the re-entrant corner slab from seismic damage since it is very susceptible to it. A typical 5th-floor slab stress concentration scenario for a 10-story building is shown in Figure 31.

Table 7 Maximum normal stress at re-entrant corner slab

Storey	Seismic Zone	Maximum normal stress at re-entrant corner slab (Psi)	Observations
10	1	798.44	Acceptable
12		790.97	Acceptable
15		799.02	Acceptable
10	2	799.81	Acceptable
12		791.05	Acceptable
15		799.31	Acceptable
10	3	799.92	Acceptable
12		971.11	Acceptable
15		799.59	Acceptable
10	4	800.06	Acceptable
12		791.28	Acceptable
15		799.76	Acceptable

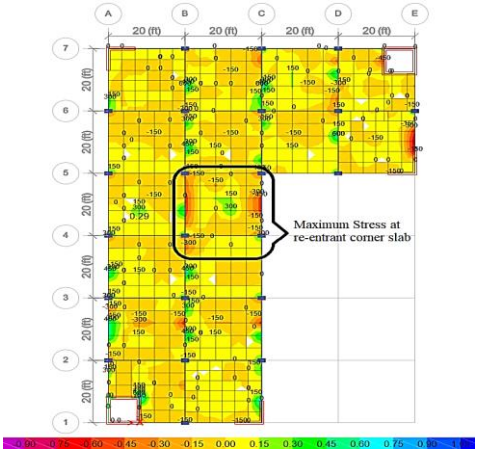

Figure 32 Normal stress observation at re-entrant corner slab (10-storey, 5F, zone 0

4.9 Centre of rigidity, Centre of Mass and Eccentricity

The center of mass is a location where mass is evenly distributed in all directions, unaffected by the gravitational field. Conversely, the center of gravity is a point within an object where weight distribution is uniform in all directions, and it is influenced by the gravitational field. Table 8 and 9 shows the Centre of gravity, Centre of mass and Eccentricity and Figure 33 illustrated the center of rigidity of the following structure.

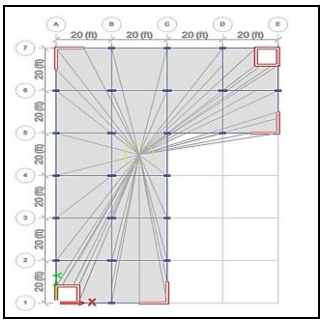

Figure 33 Center of Rigidity of the structure

Table 8 Centre of gravity and Centre of mass at different floors

Stoery	Diaphragms	Mass X (kip)	Mass Y (kip)	XCM (ft)	YCM (ft)	Cumulative X (Kip)	Cumulative Y (Kip)	XCCM (ft)	YCCM (ft)	XCR (ft)	YCR (ft)
1F	D1	42.23	42.23	30.55	69.45	42.23	42.23	30.55	69.45	38.82	64.05
2F	D2	42.23	42.23	30.55	69.45	42.23	42.23	30.55	69.45	38.33	64.12
3F	D3	42.23	42.23	30.55	69.45	42.23	42.23	30.55	69.45	37.98	64.27
4F	D4	42.23	42.23	30.55	69.45	42.23	42.23	30.55	69.45	37.70	64.43
5F	D5	42.23	42.23	30.55	69.45	42.23	42.23	30.55	69.45	37.47	64.57
6F	D6	42.23	42.23	30.55	69.45	42.23	42.23	30.55	69.45	37.27	64.70
7F	D7	42.23	42.23	30.55	69.45	42.23	42.23	30.55	69.45	37.09	64.82
8F	D8	42.23	42.23	30.55	69.45	42.23	42.23	30.55	69.45	36.93	64.92
9F	D9	42.23	42.23	30.55	69.45	42.23	42.23	30.55	69.45	36.78	65.01
10F	D10	42.23	42.23	30.55	69.45	42.23	42.23	30.55	69.45	36.65	65.09
11F	D11	42.23	42.23	30.55	69.45	42.23	42.23	30.55	69.45	36.53	65.17
12F	D12	42.23	42.23	30.55	69.45	42.23	42.23	30.55	69.45	36.42	65.24
13F	D13	42.23	42.23	30.55	69.45	42.23	42.23	30.55	69.45	36.32	65.30
14F	D14	42.23	42.23	30.55	69.45	42.23	42.23	30.55	69.45	36.24	65.35
Roof	D15	41.76	41.76	30.27	69.54	41.76	41.76	30.27	69.54	36.17	65.40

Table 9 Eccentricity check

Eccentricity		Dimension		ex/Dx result		ey/Dy result	
e_x (ft)	e_y (ft)	D_x (ft)	D_y (ft)	%		%	
8.27	5.41	80	120	10.33	Ok	4.51	Ok
7.78	5.33	80	120	9.73	Ok	4.44	Ok
7.43	5.18	80	120	9.29	Ok	4.32	Ok
7.15	5.03	80	120	8.94	Ok	4.19	Ok
6.92	4.88	80	120	8.65	Ok	4.07	Ok
6.71	4.75	80	120	8.39	Ok	3.96	Ok
6.54	4.63	80	120	8.17	Ok	3.86	Ok

Eccentricity		Dimension		ex/Dx result		ey/Dy result	
6.38	4.53	80	120	7.97	Ok	3.78	Ok
6.23	4.44	80	120	7.79	Ok	3.70	Ok
6.10	4.36	80	120	7.63	Ok	3.63	Ok
5.98	4.29	80	120	7.48	Ok	3.57	Ok
5.87	4.22	80	120	7.34	Ok	3.51	Ok
5.77	4.16	80	120	7.21	Ok	3.46	Ok
5.69	4.10	80	120	7.11	Ok	3.42	Ok
5.90	4.14	80	120	7.37	Ok	3.45	Ok
			Max	**10.3**	**Max**	**4.5**	**Ok**

4.0 CONCLUSION

It may concluded from the study that the maximum drift occurs in the middle of the building, with ESA displaying greater story drifts than RSA in both X and Y directions. Additionally, X-direction drifts exceed Y-direction drifts, with ESA surpassing RSA by 11.65%, 15.77%, and 22.39% for 10, 12, and 15-story buildings, respectively. According to the 2020 BNBC, all results remain within permissible limits. Moreover, the total base shear increases with taller buildings, and it's observed that the base shear is affected by the zoning coefficient value. It's been shown that ESA exhibits greater overturning moments than RSA in different seismic zones as building height increases. Total overturning moments vary across all zones and building heights. Seismic zone coefficients and building height have been found to influence these overturning moments. For 10, 12, and 15-story buildings, RSA overturning moments are consistently lower than ESA, by 0.94%, 2.46%, and 5.74%, respectively. Time period increases with height, with RSA exhibiting the maximum time period. For buildings up to 10, 12, and 15 stories, RSA time period exceeds ESA by 1.33%, 1.1%, and 1.79%, respectively, in the 1st mode. It also found that all re-entrant corner columns have the highest axial force when compared to similar-type columns. Compared to other types of columns, re-entrant corner columns have been shown greater rebar requirements. During the comparison of beam moments and torsion, the re-entrant corner beam displayed the highest bending moment and torsion for all seismic zones. The maximum stress is found in re-entrant corner slabs for all seismic zones.

Wind load is not taken into account in this study. Wind loads may be incorporated in future studies. Accidental torsion is not counted during analysis in this study which should be counted for future study.

Conflicts of Interest

The author(s) declare(s) that there is no conflict of interest regarding the publication of this paper.

Acknowledgement

The Ahsanullah University of Science and Technology, Tejgaon Industrial Area, Dhaka, Bangladesh, provided financial support for this work, which the authors gratefully thank. The researchers thank everyone who contributed to the study's execution. The authors express their sincere appreciation for the assistance, direction, and guidance provided by their distinguished supervisor, Dr. Sharmin Reza Chowdhury, Professor at the Department of Civil Engineering at Ahsanullah University of Science and Technology.

References

[1] Shehata, E. Abdel Raheem, M. M.-S. 2018. Seismic Performance of L-shaped Multi-storey Buildings with Moment-resisting Frames. *Proceedings of the Institution of Civil Engineers -Structures and Buildings.* 171: 395-408. Doi: https://doi.org/10.1680/jstbu.16.00122.

[2] Abdel Raheem, S. E., Ahmed, M. M. M., Ahmed, M. M. *et al.* 2018. Evaluation of Plan Configuration Irregularity Effects on Seismic Response Demands of L-shaped MRF Buildings. *Bull Earthquake Eng.* 16: 3845-3869 https://doi.org/10.1007/s10518-018-0319-7.

[3] Bohara, B. K., Ganaie, K. H., & Saha, P. 2021. Effect of Position of Steel Bracing in L-shape Reinforced Concrete Buildings under Lateral Loading. *Research on Engineering Structures & Materials.* https://doi.org/10.17515/resm2021.295st0519.

[4] A. Rahman. 2016. Understanding Earthquakes in Bangladesh. The Daily Star, Dhaka.

[5] D. Giardini. 1999. The Global Seismic Hazard Assessment Program (GSHAP) - 1992/1999. *Annals of Geophysics.* 42.

[6] S. Zawad. 2023. bHome. [Online]. Available: https://www.bproperty.com/blog/bangladesh-national-building-code/#:~:text=The%20Bangladesh%20National%20Building%20Code%20(BNBC)%20was%20first%20published%20in,1952%2C%20during%20the%20Pakistan%20era.

[7] Ahmed, M. M. M., Raheem, S. E. A., Ahmed, M. M., and Abdul-Shafy, A. G. A. 2016. Irregularity Effects on the Seismic Performance of L-shaped Multi-storey Building. *JES.* Assiut University, Faculty of Engineering. 44(5): 513-536.

[8] Abdullah, M. 2020. Assessment of Seismic Response of Vertically Irregular RC Moment Resisting Frame Structures. M.Sc. Thesis. Bangladesh University of Engineering and Technology, Bangladesh.

[9] J. Hammer. 2011. The Great Japan Earthquake of 1923. [Online]. Available: https://www.smithsonianmag.com/history/the-great-japan-earthquake-of-1923-1764539/.

[10] Ahmadi, M. N. J., and Sanghvi, C. S. 2017. Comparative Study of Response of Irregular Structures and Effect of Shear Walls on Irregular Buildings. *International Journal of Advanced Research.* 5(2): 1715-1724.

[11] B. S. s. S. S. Shreyasvi. C. 2015. A Case Study on Seismic Response of Buildings with Re-entrant Corners. *International Journal of Engineering Research & Technology (IJERT).* 1071-1078.

[12] WIKIMEDIA. 2023. File:1985 Mexico Earthquake - Ministry of Telecommunications and Transportation Building 4.jpg. Wikimedia Coomons.
[13] B. A. A. D. T. G. N. Lohith Kumar, B. C. 2017. Seismic Effect of Re-entrant and Torsional Irregularities on Multi-storey Buildings. *International Research Journal of Engineering and Technology (IRJET)*. 4(4).
[14] S. B. Ankon. 2020. A Comparative Study of Behavior of Multi-Storied Regular and Irregular Buildings under Static and Dynamic Loading. *Open Journal of Civil Engineering*. 337-352.
[15] Farhan, M. A. A., and Bommisetty, J. 2019. Seismic Analysis of Multistoried RCC Buildings Regular and Irregular in Plan. *International Journal of Engineering Research & Technology (IJERT)*. 8(11).
[16] Herrera, G. R., and Soberón, G. C. 2008. Influence of Plan Irregularity of Building. *14th World Conference on Earthquake Engineering, Beijing, China.*
[17] Kakpure, G. G., and Mundhada, A. R. 2019. Comparative Study of Static and Dynamic Seismic Analysis of Multistoried RCC Building by ETABS: A Review. *International Journal of Emerging Research in Management & Technology*. 5(12).
[18] Kalambe, Y. K., and Denge, S. 2019. Seismic Analysis of R.C.C. Building with Plan Irregularities. *International Journal for Science and Advance Research in Technology*. 5(6).
[19] Mohiuddin, M. A., and Singh, B. 2019. Seismic Vulnerability Assessment of Irregular RCC Buildings by Considering the Effect of Shear Walls. *International Journal of Engineering Research and Applications.* 9(7).
[20] Monish, S., and Karuna, S. 2015. A Study on Seismic Performance of High Rise Irregular RC Framed Buildings. *International Journal of Research in Engineering and Technology*.
[21] Shakib, H., & Fuladgar, A. 2004. Dynamic Soil–structure Interaction Effects on the Seismic Response of Asymmetric Buildings. *Soil Dynamics and Earthquake Engineering*. 24(5): 379-388. https://doi.org/10.1016/j.soildyn.2004.01.002.
[22] Patil, S. S., and Suryawanshi, S. R. 2016. A Study of Plan Irregularity Inducing Accidental Torsional Moment of Multi-story Building using Stadd Pro. *International Journal of Current Engineering and Technology*.
[23] Zia, F. M., and Banerjee, R. 2020. Seismic Impact of Re-entrant Corner with Opening in Diaphragm on RC Building. *International Journal of Recent Technology and Engineering*. 9(1).